How to cite: *Angew. Chem. Int. Ed.* **2021**, *60*, 19740–19743
International Edition: doi.org/10.1002/anie.202106337
German Edition: doi.org/10.1002/ange.202106337

Borosulfates | Hot Paper

Triple-Vertex Linkage of (BO_4)-Tetrahedra in a Borosulfate: Synthesis, Crystal Structure, and Quantum-Chemical Investigation of $Sr[B_3O(SO_4)_4(SO_4H)]$

*Leonard C. Pasqualini, Hubert Huppertz, Minyeong Je, Heechae Choi, and Jörn Bruns**

Abstract: *Borosulfates are classified as silicate analogue materials. The number of crystallographically characterized compounds is still limited, whereas the structural diversity is already impressive. The anionic substructures of borosulfates exhibit vertex-connected (BO_4)- and (SO_4)-tetrahedra, whereas bridging between two (SO_4)- or even between two (BO_4)-tetrahedra is scarce. The herein presented compound $Sr[B_3O(SO_4)_4(SO_4H)]$ is the first borosulfate with a triple-vertex linkage of three (BO_4) tetrahedra via one common oxygen atom. DFT calculations complement the experimental studies. Bader charges (calculated for all atoms) as well as charge-density calculations give hint to the electron distribution within the anionic substructure and density-of-states calculations support the interpretation of the bonding situation.*

Mainly, borosulfates are known as glasses.[1] However, elucidation of their crystal structures gained increasing interest for several applications like solid acid polyelectrolytes or NLO materials during the recent years.[2] Up to now, the number of structurally characterized borosulfates is low compared to silicates. Still, the structural diversity is already impressive. The anionic substructures of borosulfates are similar to silicates, exhibiting *soro-, neso-, cyclo-*, *ino-*, *phyllo-*, and *tectosilicates* like topologies of vertex connected (BO_4)- and (SO_4)-tetrahedra.[3] Even the formation of S-O-S[3b,c,e,4,5] and B-O-B[3i,6–9] bonds is not uncommon. This finding is in contrast to the structures of alumosilicates, wherein Al-O-Al bonds are not to be expected according to Loewenstein's rule.[10] However, also for borosulfates only vertex linkage of two (SO_4)- or (BO_4)-tetrahedra, resulting in the formation of (S_2O_7)- and (B_2O_7)-subunits, is known.

Recently, Höppe and co-workers reported on $Mg_3[H_2O \rightarrow B(SO_4)_3]_2$, exhibiting a *Lewis*-acid-base adduct of water to a $[B(SO_4)_3]^{3-}$ moiety.[11] The latter was obtained from a reaction of $MgCO_3$ and H_3BO_3 with sulfuric acid and low amounts of SO_3 at moderate temperature of 453 K. Accordingly, the reaction conditions play a crucial rule for the constitution and topology of the anionic substructures. This has also been shown for the three different structurally characterized strontium borosulfates $Sr[B_2(SO_4)_3](S_2O_7)]$,[4] $Sr[B_2(SO_4)_4]$,[3h] and $Sr[B_2O(SO_4)_3]$.[9] Especially the reaction temperature (T_{max}) and time as well as the SO_3 content of the starting materials have a significant influence on the B:S ratio and the topology of the anionic network. $Sr[B_2(SO_4)_4]$, exhibiting loop branched *vierer* single chains with S-O-B bridges exclusively, was synthesized from a 1:4 mixture of sulfuric acid and oleum (65 % SO_3) at $T_{max} = 453$ K. The same product can be obtained by using only oleum (65 % SO_3) instead of a mixture with sulfuric acid. By reducing the time at T_{max} from 24 h to 12 h for the same reaction $Sr[B_2(SO_4)_3](S_2O_7)]$ is formed instead. The anionic substructure of $Sr[B_2(SO_4)_3](S_2O_7)]$ reveals loop-branched *vierer* double chains and exhibits besides S-O-B also S-O-S bridges. The synthesis of $Sr[B_2O(SO_4)_3]$ involves a pre-reaction of sulfuric acid with boric acid, followed by a long tempering period (96 h) at a high T_{max} of 573 K of the mixture with oleum (65 % SO_3) and the strontium precursor. The anionic substructure of $Sr[B_2O(SO_4)_3]$ reveals a chain-like arrangement of the fundamental building block and B-O-B bridges. In our opinion, the increased temperature is the main reason for the formation of B-O-B bridges. By applying high temperatures, SO_3 can be released into the gaseous phase and is no longer available for the formation of S-O-B or even S-O-S bridges.

With the aim to synthesize a highly B-O-B enriched species and controlling the cation to boron ratio simultaneously, the title compound $Sr[B_3O(SO_4)_4(SO_4H)]$[12] was synthesized at a high temperature of 523 K in a specially designed setup (Figure 1; for details see experimental section in the Supporting Information). Therefore, $SrCO_3$ and boric acid were ground together and filled into a glass vial, which was placed inside a glass ampoule filled with oleum (65 % SO_3) and a glass pin as spacer. By increasing the temperature, SO_3 is transferred to the gaseous phase and was allowed to react with the solid starting material. Due to this inventive setup, the amount of reacting SO_3 remains as low as possible. The product is a colorless crystalline solid (Figure S1) and is phase-pure according to powder X-ray diffraction (Figure S2).

The anionic substructure of $Sr[B_3O(SO_4)_4(SO_4H)]$ is charge compensated by Sr^{2+} cations. The latter are coordi-

[*] Dr. M. Je, Dr. H. Choi, Dr. J. Bruns
Institute of Inorganic Chemistry, University of Cologne
Greinstrasse 6, 50939 Cologne (Germany)
E-mail: j.bruns@uni-koeln.de
M. Sc. L. C. Pasqualini, Prof. Dr. H. Huppertz
Institute of General, Inorganic, and Theoretical Chemistry, University of Innsbruck
Innrain 80–82, 6020 Innsbruck (Austria)
Supporting information and the ORCID identification number(s) for the author(s) of this article can be found under: https://doi.org/10.1002/anie.202106337.

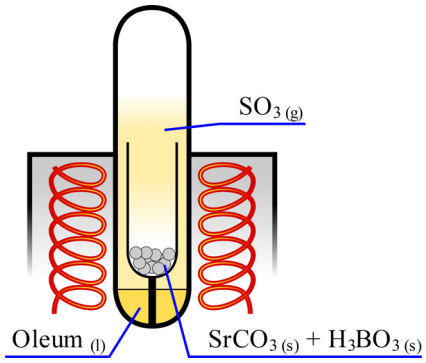

Figure 1. Schematic drawing of the experimental setup. The torch sealed ampoule, in which the solid starting material is separated from the solvent by a glass tube, is placed inside a block shaped resistance furnace.

nated by nine oxygen atoms in form of a distorted single-capped square antiprism (Figures S3 and S4).

The borosulfate anions reveal an *inosilicate* like topology of $\{B_3O(SO_4)_3(SO_4H)\}$ aggregates bridged by two (SO_4)-tetrahedra to form strongly corrugated chains (Figure 2) which run parallel to the crystallographic *b*-axis (Figure 3). Each aggregate exhibits one (SO_4H)-tetrahedron forming,

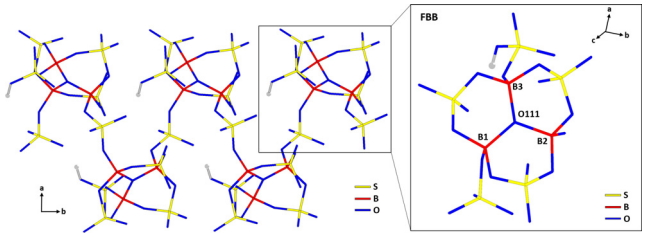

Figure 2. Left: Infinite anionic borosulfate chain in the structure of $Sr[B_3O(SO_4)_4(SO_4H)]$. The chains run parallel to the crystallographic *b*-axis; right: Cutout from the anionic chains in the structure of $Sr[B_3O(SO_4)_4(SO_4H)]$ (FBB), emphasizing the central motif of three (BO_4)-tetrahedra vertex-connected via one particular oxygen atom. B–O bond lengths [Å]: B1-O111 1.507(2), B2-O111 1.508(2), B3-O111 1.524(2).

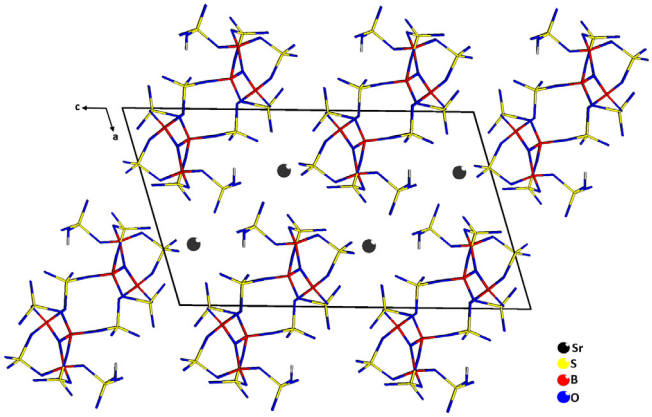

Figure 3. Crystal structure of $Sr[B_3O(SO_4)_4(SO_4H)]$. Infinite anionic chains run parallel to the crystallographic *b*-axis. The chains are separated by Sr^{2+} cations.

according to Jeffrey's classification,[13] a medium strong hydrogen bridge with donor-acceptor distances of D-(H)···A = 2.539(2) Å to a bridging (SO_4)-tetrahedron within the same chain. Three (SO_4)-tetrahedra are vertex connected to the three central (BO_4)-tetrahedra in a bidentate chelating manner, respectively. The terminal S–O bonds of the $\{B_3O(SO_4)_3(SO_4H)\}$ subunit and of the bridging (SO_4)-tetrahedra reveal values of 1.42 Å in average. The average length of the terminal S–O bonds in the (HSO_4)-tetrahedra is 1.43 Å. Obviously, the single coordination of the (SO_4H) fragment has an influence on the S–O bond and causes an elongation for the S–O bond to 1.516(2) Å. In the center of the $\{B_3O(SO_4)_3(SO_4H)\}$ aggregate resides one oxygen atom, which is the single vertex of three (BO_4)-tetrahedra. The B–O bonds to the triple coordinated oxygen atom O111 are elongated to values of 1.507(2), 1.508(2), and 1.524(2) Å compared to the B–O bonds of the B-O-S bridges with an average value of 1.46 Å (for a detailed list of bond lengths and angles see Tables S4 and S5). Compared to previous results on borosulfates,[3] the reaction temperature of the herein presented synthesis is comparably high (523 K), which leads to a high B:S ratio of 3:5, making the formation of B-O-B bonds initially possible.

The fundamental building block (FBB), which describes the anionic substructure, shows a B:S ratio of 3:5 and can be written as $8\square:[\Phi]<3\square>\square\,|\,\square<3\square>\square\,|\,\square<3\square>|$, where $[\Phi]$ stands for the bridging μ_3 oxygen atom.[14] These FBBs form the anionic chains with the Niggli formula $^1_\infty\left\{\left[(B_3O)(SO_4)_{6/2}(SO_4)_{2/2}(HSO_4)_{1/1}\right]^{2-}\right\}$.

A comparable μ_3 oxygen atom as vertex for three (BO_4)-units is found in $Ag_2(NH_4)_3[(UO_2)_2(B_3O(PO_4)_4(PO_4H)_2)]H_2O$.[15] The B–O bond lengths are similar to our findings and fall in the narrow range of 1.490(18) to 1.568(11) Å. However, in this compound the charge compensation of the heteropolyanion is achieved by multiple, partially highly charged cations. For homopolyanions, a triple vertex connection around one oxygen atom is also uncommon but not unknown. Comparable arrangements are found in *meta*-oxoborates $RE(BO_2)_3$ (RE = Dy-Lu),[16] $Sr[B_8O_{11}(OH)_4]$,[17] the heptaborate anion $[B_7O_9(OH)_5]^{2-}$[18] and the nonaborate anion $[B_9O_{16}](OH)^{6-}$.[19,20] In all mentioned examples, the B–O bond lengths fall in the same range (values around 1.5 Å). Even so, according to Pauling's 4th rule[21] the triple vertex connection remains unexpected. The latter assumption is also manifested by a recent study on around 5000 crystalline compounds, indicating that especially small main group elements fulfill Pauling's 4th rule by > 90 %.[22]

To further understand the bonding situation in the borosulfate $Sr[B_3O(SO_4)_4(SO_4H)]$, we performed density functional theory (DFT) calculations. The theoretical electron density of states (DOS) reveals a band gap of 8.5 eV (Figure 4), which is consistent with the transparency of the single crystals and similar to the finding for $Sr[B_2O(SO_4)_3]$ (9.6 eV).[9] The uppermost valence band (VBM) and the lowest conduction band (CBM) mostly consist of p-orbitals of oxygen atoms and s-orbitals of sulfur atoms, respectively.

It is noticeable that the theoretical Bader charge of the oxygen atom coordinated to three boron atoms (O111) is

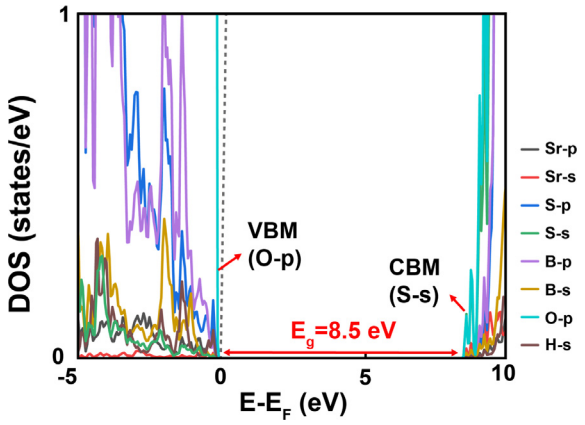

Figure 4. Calculated electron density of states (DOS) of $Sr[B_3O(SO_4)_4(SO_4H)]$ using DFT with the HSE06 functional.[23] The calculated Bader charges of the different atoms in $Sr[B_3O(SO_4)_4(SO_4H)]$ are depicted in Figure 5.

1.18e, and the oxygen atoms bound to a sulfur atom and a boron atom (for example O12) have a Bader charge of 1.13e (Figure 5). The larger Bader charge of O111 (1.18e) than that of O12 (1.13e) can be explained with the small occupation of anti-bonding states below the Fermi energy, as shown in the calculated projected crystal orbital Hamiltonian population (-pCOHP)[24] of Figure 6b. The slightly lower Bader charge on O12 is due to the more antibonding nature of the chemical bond leading to a higher degree of electron delocalization towards the S atom compared to the O–B bond in the case of the B_3O unit containing the O111 atom.

The O12 atom has σ-bonds with boron and sulfur atoms as shown in the computed partial charge densities at the largest -pCOHP peaks (numbered 1 in Figure 6a). Furthermore, there is electron density located in p_y and p_z-orbitals near the Fermi energy that contributes almost equally to bonding and antibonding (numbered 2 in Figure 6a). As can be seen from the calculated -pCOHP, the p_z-orbital of O12 atom has major contribution to the antibonding among all the calculated

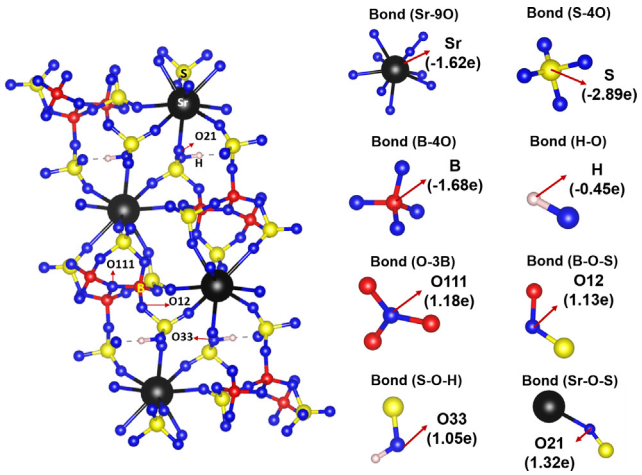

Figure 5. Crystal structure of $Sr[B_3O(SO_4)_4(SO_4H)]$ (left) and the calculated Bader charge for each atom (right).

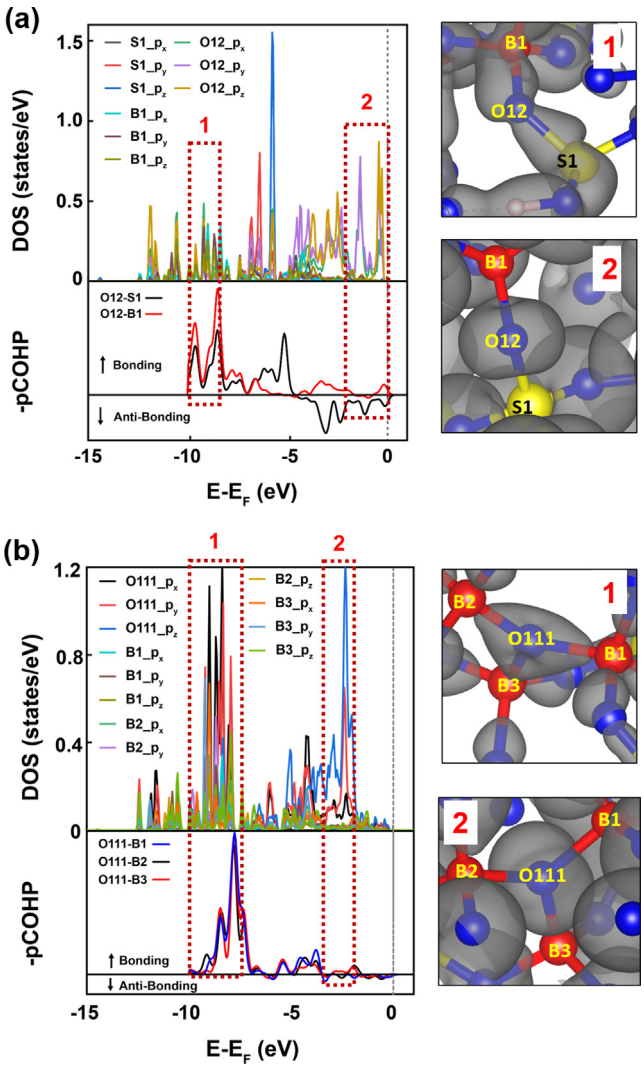

Figure 6. Calculated electron density of states (DOS), -pCOHP, and the partial charge densities (grey surfaces in the right panels) for oxygen atoms coordinated with (a) one boron, one sulfur atom (O12) and (b) three boron atoms (O111). The red, blue, and yellow spheres are boron, oxygen, and sulfur atoms, respectively. The isovalue of the partial charge density isosurfaces was set to 0.1 eÅ^{-3}.

electron orbitals (the largest peak is −3.4 eV below the Fermi energy).

The partial charge densities of the atom O111 shows that it has σ-bonds with the surrounding boron atoms (numbered 1 in Figure 6b). Furthermore, this atom has significant amount of electron density near the Fermi level, as indicated by the localized p_z-orbital (partial charge density in range 2 of Figure 6b), but nearly-zero bonding/antibonding state (see -pCOHP). Overall, the amount of antibonding is less pronounced for O111 than for O12.

The afore presented results shed new light on the structure family of borosulfates. Hitherto, borosulfates were often discussed in the context of silicates. Accordingly, the anionic substructure resembles a substitution variant like alumosilicates. However, the formation of S-O-S and B-O-B bridges in some borosulfates is already contrary to the typical trends in silicate chemistry, like the Loewenstein rule. The

triple vertex connection of three (BO_4)-tetrahedra in the structure of $Sr[B_3O(SO_4)_4(SO_4H)]$ outperforms this silicate untypical behavior. Rather, the structure reflects a typical motif of borate chemistry. To the best of our knowledge, the formation of this unique compound is only possible via a smart synthesis strategy.

Since we have been able to describe the greatest similarity of a borosulfate to borates so far, the question now arises whether we can push it even further and possibly even realize the structural motif of two edge-sharing (BO_4)-tetrahedra inside a borosulfate. Although, this motif might be found under normal pressure conditions, we will also try to realize such an arrangement under high-pressure conditions, where the feasibility is much higher.

Acknowledgements

Jörn Bruns is thankful for the financial support by the Fonds der Chemischen Industrie (FCI). We thank Assoz.-Prof. Dr. Gunter Heymann and Ass.-Prof. Dr. Klaus Wurst for the collection and the evaluation of the X-ray data, respectively. Minyeong Je and Heechae Choi acknowledge the financial support of Federal Ministry of Education and Research (BMBF) under the "Make Our Planet Great Again—German Research Initiative" (MOPGA-GRI), 57429784, implemented by the German Academic Exchange Service Deutscher Akademischer Austauschdienst (DAAD). Leonard C. Pasqualini thanks the University of Innsbruck for a PhD scholarship. Open access funding enabled and organized by Projekt DEAL.

Conflict of Interest

The authors declare no conflict of interest.

Keywords: borosulfates · charge-density calculations · density functional theory · density of states · solvothermal synthesis

[1] O. Mustarelli, S. Scotti, M. Villa, P. R. Gandhi, *Solid State Ionics* **1990**, *39*, 217 – 224.
[2] a) L. Kang, X. Liu, Z. Lin, B. Huang, *Phys. Rev. B* **2020**, *102*, 205424; b) M. D. Ward, B. L. Chaloux, M. D. Johannes, A. Epshteyn, *Adv. Mater.* **2020**, *32*, 2003667; c) Y. Li, Z. Zhou, S. Zhao, F. Liang, Q. Ding, J. Sun, Z. Lin, M. Hong, J. Luo, *Angew. Chem. Int. Ed.* **2021**, *60*, 11457 – 11463; *Angew. Chem.* **2021**, *133*, 11558 – 11564.
[3] a) H. A. Höppe, K. Kazmierczak, M. Daub, K. Förg, F. Fuchs, H. Hillebrecht, *Angew. Chem. Int. Ed.* **2012**, *51*, 6255 – 6257; *Angew. Chem.* **2012**, *124*, 6359 – 6362; b) M. Daub, K. Kazmierczak, P. Gross, H. Höppe, H. Hillebrecht, *Inorg. Chem.* **2013**, *52*, 6011 – 6020; c) M. Daub, H. A. Höppe, H. Hillebrecht, *Z. Anorg. Allg. Chem.* **2014**, *640*, 2914 – 2921; d) J. Bruns, M. Podewitz, O. Janka, R. Pöttgen, K. Liedl, H. Huppertz, *Angew. Chem. Int. Ed.* **2018**, *57*, 9548 – 9552; *Angew. Chem.* **2018**, *130*, 9693 – 9697; e) M. Daub, K. Kazmierczak, H. A. Höppe, H. Hillebrecht, *Chem. Eur. J.* **2013**, *19*, 16954 – 16962; f) J. Bruns, M. Podewitz, M. Schauperl, K. Liedl, O. Janka, R. Pöttgen, H. Huppertz, *Eur. J. Inorg. Chem.* **2017**, 3981 – 3989; g) S. Schönegger, J. Bruns, B. Gartner, K. Wurst, H. Huppertz, *Z. Anorg. Allg. Chem.* **2018**, *644*, 1702 – 1706; h) P. Netzsch, H. A. Höppe, *Z. Anorg. Allg. Chem.* **2020**, *646*, 1563 – 1569; i) P. Netzsch, P. Gross, H. Takahashi, H. A. Höppe, *Inorg. Chem.* **2018**, *57*, 8530 – 8540; j) J. Bruns, M. Podewitz, M. Schauperl, B. Joachim, K. Liedl, H. Huppertz, *Chem. Eur. J.* **2017**, *23*, 16773 – 16781; k) L. C. Pasqualini, O. Janka, S. Olthof, H. Huppertz, K. Liedl, M. Podewitz, J. Bruns, *Chem. Eur. J.* **2020**, *26*, 17405 – 17415; l) P. Netzsch, F. Pielnhofer, R. Glaum, H. A. Höppe, *Chem. Eur. J.* **2020**, *26*, 14745 – 14753; m) M. Hämmer, L. Bayarjargal, H. A. Höppe, *Angew. Chem. Int. Ed.* **2021**, *60*, 1503 – 1506; *Angew. Chem.* **2021**, *133*, 1525 – 1529.
[4] P. Netzsch, H. A. Höppe, *Inorg. Chem.* **2020**, *59*, 18102 – 18108.
[5] P. Netzsch, H. A. Höppe, *Eur. J. Inorg. Chem.* **2020**, 1065 – 1070.
[6] P. Gross, A. Kirchhain, H. A. Höppe, *Angew. Chem. Int. Ed.* **2016**, *55*, 4353 – 4355; *Angew. Chem.* **2016**, *128*, 4426 – 4428.
[7] C. Logemann, M. S. Wickleder, *Angew. Chem. Int. Ed.* **2013**, *52*, 14229 – 14232; *Angew. Chem.* **2013**, *125*, 14479 – 14482.
[8] M. Daub, H. Hillebrecht, *Eur. J. Inorg. Chem.* **2015**, 4176 – 4181.
[9] P. Netzsch, P. Gross, H. Takahashi, S. Lotfi, J. Brgoch, H. A. Höppe, *Eur. J. Inorg. Chem.* **2019**, 3975 – 3981.
[10] W. Loewenstein, *Am. Mineral.* **1954**, *39*, 92 – 96.
[11] P. Netzsch, R. Stroh, F. Pielnhofer, I. Krossing, H. A. Höppe, *Angew. Chem. Int. Ed.* **2021**, *60*, 10643 – 10646; *Angew. Chem.* **2021**, *133*, 10738 – 10741.
[12] CSD number 2078352.
[13] G. A. Jeffrey, *An Introduction to Hydrogen Bonding*, Oxford University Press, Oxford, **1997**.
[14] P. C. Burns, J. D. Grice, F. C. Hawthorne, *Can. Mineral.* **1995**, *33*, 1131 – 1151.
[15] S. Wu, M. J. Polinski, T. Malcherek, U. Bismayer, M. Klinkenber, G. Modolo, D. Bosbach, W. Depmeier, T. E. Albrecht-Schmitt, E. V. Alekseev, *Inorg. Chem.* **2013**, *52*, 7881 – 7888.
[16] H. Emme, T. Nikelski, T. Schleid, R. Pöttgen, M. H. Möller, H. Huppertz, *Z. Naturforsch. B* **2004**, *59*, 202 – 215.
[17] A. A. Brovkin, N. V. Zayakina, V. S. Brovkina, *Kristallografiya* **1975**, *20*, 911 – 916.
[18] D. M. Schubert, M. Z. Visl, S. Khan, C. B. Knobler, *Inorg. Chem.* **2008**, *47*, 4740 – 4745.
[19] E. L. Belokoneva, S. Stefanovich, T. A. Borisova, O. V. Dimitrova, *Zh. Neorg. Khim.* **2001**, *46*, 1788 – 1794.
[20] E. L. Belokoneva, S. Y. Stefanovich, O. V. Dimitrova, N. N. Mochenova, N. V. Zubkova, *Crystallogr. Rep.* **2009**, *54*, 814 – 821.
[21] L. Pauling, *J. Am. Chem. Soc.* **1929**, *51*, 1010 – 1026.
[22] J. George, D. Waroquiers, D. Di Stefano, G. Petretto, G.-M. Rignanese, G. Haultier, *Angew. Chem. Int. Ed.* **2020**, *59*, 7569 – 7575; *Angew. Chem.* **2020**, *132*, 7639 – 7645.
[23] J. Heyd, G. E. Scuseria, *J. Chem. Phys.* **2003**, *118*, 8207 – 8215.
[24] a) S. Maintz, V. L. Deringer, A. L. Tchougréeff, R. Dronskowski, *J. Comput. Chem.* **2016**, *37*, 1030 – 1035; b) V. L. Deringer, A. L. Tchougréeff, R. Dronskowski, *J. Phys. Chem. A* **2011**, *115*, 5461 – 5466.

Manuscript received: May 11, 2021
Revised manuscript received: June 4, 2021
Accepted manuscript online: June 13, 2021
Version of record online: July 9, 2021

